JOURNAL OF APPLIED ELECTROCHEMISTRY 22 (1992) 865–871

Electrochemical reduction of Eu(III) using a flow-through porous graphite electrode

T. M. HUNG, C. J. LEE*

Department of Chemical Engineering, National Tsing Hua University, Hsinchu, Taiwan

Received 15 April 1991; revised 1 December 1991

Divalent europium ions were produced from trivalent lanthanide solution by using a flow-through porous graphite electrode. The reduction of Eu(III) was investigated by varying the composition of electrolyte, flow rate and applied current in an electrochemical system with recycle. Increasing the ratio of lanthanide to europium content and the flow rate favoured the rate of reduction and improved the efficiency. High current efficiency was obtained by applying high current. Evolution of hydrogen and reoxidation of the reduced europium caused reduction in the current efficiency. A mathematical model was developed to describe the electrochemical system, the values obtained from the model computation compared closely with experimental results.

Nomenclature

- a specific surface area of the electrode ($cm^2\,cm^{-3}$)
- A geometrical cross-sectional area of the electrode (cm^2)
- $C(x, t)$ reactant concentration at electrode position x and instant time t ($mol\,cm^{-3}$)
- C' product concentration ($mol\,cm^{-3}$)
- E^0 electrode potential (V)
- f ratio factor
- F Faraday's constant ($96\,487\,C\,mol^{-1}$)
- i subscript noted as initial state
- I_a applied cell current (A)
- I_L limiting current (A)
- J mass flux from bulk electrolyte to electrode ($mol\,cm^{-2}\,s^{-1}$)
- k rate constant of the zero order reaction ($mol\,cm^{-3}\,s^{-1}$)
- k_a apparent mass transfer coefficient, $k_m a$ (s^{-1})
- k_m mass transfer coefficient ($cm\,s^{-1}$)
- L electrode thickness (cm)
- Q flow rate of electrolyte ($cm^3\,s^{-1}$)
- R chemical reaction rate ($mol\,cm^{-3}\,s^{-1}$)
- R_t conversion factor, $R_t = 1 - \exp(-k_m aAL/Q)$
- T superscript noted as total Eu
- TRE total rare earths (lanthanides) concentration (M)
- t instant time (s)
- u electrolyte flow velocity, $u = Q/A$ ($cm\,s^{-1}$)
- V volume of reservoir (cm^3)
- x geometrical location of the electrode
- ε porosity of the electrode
- $\bar{\eta}$ overall mean current efficiency, (Equation 11)
- τ residence time, V/Q (s)

1. Introduction

Flow-through porous electrodes which provide a large specific surface area have attracted much interest in electrochemical processing. A review article on this subject has been published [1]. Of considerable interest is the use of this electrode system for removal of metal ions and chelating agents from waste water [2] and charging and discharging of zinc–chlorine batteries [3, 4]. Although the electrochemical reduction of europium had been discussed very early in the literature, there were only a few studies reported on the reduction of europium using flow-through porous electrodes. Inert porous carbon electrodes were first selected for europium reduction from a mixture of lanthanides in a bromide medium [5]. Recently, membrane-partitioned flow-through porous graphite electrodes were used to carry out the reduction of europium [6, 7]. Between the two graphite sheets, an anion exchange membrane was clamped. The trivalent europium was reduced in such a redox cell; subsequently, the divalent europium was separated from trivalent lanthanides by precipitation of europous sulphate.

In the present study, a model reactor based on the concept of membrane-partitioned flow-through porous graphite electrodes was designed to carry out the reduction of europium. The europium chloride catholyte and the ferrous chloride anolyte were continuously recycling through the corresponding electrodes. The reduction rate of europium and the depletion of ferrous ion were investigated by varying the system parameters, including flow rate, applied current and the composition of electrolyte. A

* Correspondence concerning this paper should be addressed to T. M. Hung, Chemical Engineering Division, Institute of Nuclear Energy Research, Lung-Tan, Taiwan.

0021-891X/92

mathematical model was also formulated to describe the electroreduction performance characteristics and to compare with the experimental results.

2. Theory

2.1. *Redox potentials*

Of the fifteen lanthanide elements, there are only three (samarium, europium and ytterbium) whose valence state may be changed. The M^{3+}/M^{2+} redox potentials are -1.55, -0.43 and -1.15 V for samarium, europium and ytterbium, respectively. The potential for europium is relatively small compared with those for the other two. By applying a moderate potential, divalent europium may be obtained exclusively through the electrolysis of trivalent lanthanide mixtures without the formation of divalent samarium and ytterbium. In the electrolytic cell used here, europium chloride solution and ferrous chloride solution served as the catholyte and the anolyte, respectively. The following electrode reactions may be involved:

$$\textit{Cathode}\ H^+ + e^- \longrightarrow \tfrac{1}{2}H_2 \qquad E^0 = 0.00\,V \tag{1}$$

$$Eu^{3+} + e^- \longrightarrow Eu^{2+} \qquad E^0 = -0.43\,V \tag{2}$$

$$\textit{Anode}\ Fe^{2+} \longrightarrow Fe^{3+} + e^- \qquad E^0 = -0.77\,V \tag{3}$$

If what is required is the cell potential for the redox reaction alone, then the equilibrium form of the Nernst equation may be formulated:

$$E = -1.20 - 0.059 \log \frac{[Eu^{2+}][Fe^{3+}]}{[Eu^{3+}][Fe^{2+}]} \tag{4}$$

It is obvious that $[Eu^{3+}]$ and $[Fe^{2+}]$ would decrease while $[Eu^{2+}]$ and $[Fe^{3+}]$ increase during the process; and the applied voltage must be increased to maintain the driving force to keep the redox reaction proceeding. However, it is undesirable but inevitable that hydrogen evolution will take place simultaneously with europium reduction at the cathode, because the europium is less noble than hydrogen.

Divalent europium in aqueous solution is extremely unstable and can easily be photo-oxidized [8] in water:

$$Eu^{2+}(H_2O) \xrightarrow{250,325\,nm} Eu^{3+} + H^{\cdot} + OH^- \tag{5}$$

Also, in the presence of oxygen, divalent europium can be rapidly reoxidized with acid [9],

$$Eu^{2+} + H^+ + \tfrac{1}{4}O_2 \longrightarrow Eu^{3+} + \tfrac{1}{2}H_2O \tag{6}$$

These photochemical and/or chemical electron exchange reactions increase the complexity of the electrochemical system.

2.2. *Mathematical model*

The basic assumptions involved in the development of the mathematical model are: (i) that the porous electrode is of uniform porosity and specific surface area; (ii) that idealized plug flow exists in the porous electrode; (iii) that the reservoir is perfectly mixed; (iv) that the mass transfer coefficient is constant throughout the reactor; and finally (v) that the physical properties of the electrolyte remain constant with time.

During the recycling mode of operation, the chemical reoxidation of divalent europium in the cell was ignored because of the shorter residence time in the cell relative to that in the reservoir. The reactant concentration, C, in the porous electrode is a function of both position, x and time, t. The mass-conservation equation may be written

$$\varepsilon \frac{C(x, t)}{t} + u \frac{C(x, t)}{x} + aJ = 0 \tag{7}$$

For the reservoir, the equation for the change of concentration with time is

$$\tau \frac{C(0, t)}{t} = C(L, t) - C(0, t) + \tau R \tag{8}$$

where, $C(L, t)$ and $C(0, t)$ are the concentrations at the outlet ($x = L$) and the inlet ($x = 0$) of the electrode, respectively. Walker and Wragg [10] have solved the above equations without the chemical reaction term by means of the Laplace transform method. The complete solution of Equations 7 and 8 with chemical reaction is rather complicated. For practical purposes, an approximate yet satisfactory solution may be obtained by assuming that the reactor is at steady-state and the rate of reoxidation in the reservoir is zero order with respect to divalent europium. Based on the relative magnitude of the applied current, I_a, and the limiting current, I_L, two cases are discussed as follows.

Case I: The electrochemical condition, $I_a < I_L$

For an electroreduction accompanied by hydrogen evolution, there is a ratio factor f between the effective current and the applied current, which represents the effective conversion of the desired reactive ions. For the sake of simplification, the factor f is assumed to be independent of time, if the limiting reactant is a minor constituent. Thus, the flux can be expressed

$$J = \frac{fI_a}{FaAL} \tag{9}$$

and the steady state concentration of electrolyte at $x = L$ is obtained by integrating Equation 7,

$$C(L, t) = C(0, t) - \frac{fI_a}{FQ} \tag{10}$$

Integration of Equation 8 using the value of $C(L, t)$ from Equation 10 leads to a solution of the concentration of product ions (i.e. divalent europium ions) C' in the reservoir as a function of time:

$$\frac{C'(0, t)}{C(0, 0)} = \frac{1}{C(0, 0)}\left(\frac{fI_a}{FV} - k\right)t \tag{11}$$

The mean current efficiency over the period between the initial time and the instant t is defined by the following

$\bar{\eta}$ = Increase in mass of product species in reservoir/Mass of product species equivalent to electricity consumed (12)

Using this definition, the mean current efficiency becomes

$$\bar{\eta} = \frac{C'(0, t)FV}{I_a t} \quad (13)$$

Combining Equations 11 and 13 leads to a further expression for the mean current efficiency, i.e.

$$\bar{\eta} = f - \frac{kFV}{I_a} \quad (14)$$

Case II: The diffusional condition, $I_a > I_L$

In this case, the applied current I_a is always greater than the limiting current I_L; however the reactive ions change during the recycling operation. The rate of electroreduction becomes controlled by diffusion of ions from the bulk solution to the pore wall. Hence, the flux is generally expressed as $J = k_m C(x, t)$.

By integration of Equation 7 at steady state, the exit concentration at $x = L$ relative to the inlet concentration at $x = 0$ is given by

$$C(L, t) = C(0, t) \exp\left(-\frac{k_m aAL}{Q}\right) \quad (15)$$

By substitution of Equation 15 into Equation 8 for a zero order reoxidation and after integration, the concentration of product ions, C', in the reservoir may be obtained,

$$\frac{C'(0, t)}{C(0, 0)} = \left(1 - \frac{\tau k}{R_t C(0, 0)}\right)\left[1 - \exp\left(-\frac{R_t}{\tau} t\right)\right] \quad (16)$$

where, $R_t = 1 - \exp(-k_m aAL/Q)$ stands for the conversion factor in one passage through the porous electrode.

Following the definition of Equation 12, the mean current efficiency becomes

$$\bar{\eta} = \frac{FV}{I_a t}\left[C(0, 0) - \frac{\tau k}{R_t}\right]\left[1 - \exp\left(-\frac{R_t}{\tau} t\right)\right] \quad (17)$$

3. Experimental details

The flow scheme is shown in Fig. 1. The cell assembly is shown in Fig. 2. The porous electrodes were machined from a block of EG-NPL (Nippon Carbon Co.) graphite. Each electrode was 5 mm thick, with 88 cm^2 apparent surface area in contact with the electrolyte. Two graphite electrodes were clamped together with two acrylic frames, between which was an anion exchange membrane (IONAC MA-3475, Sybron Co.) dividing the cell into two compartments. A 4 mm thick

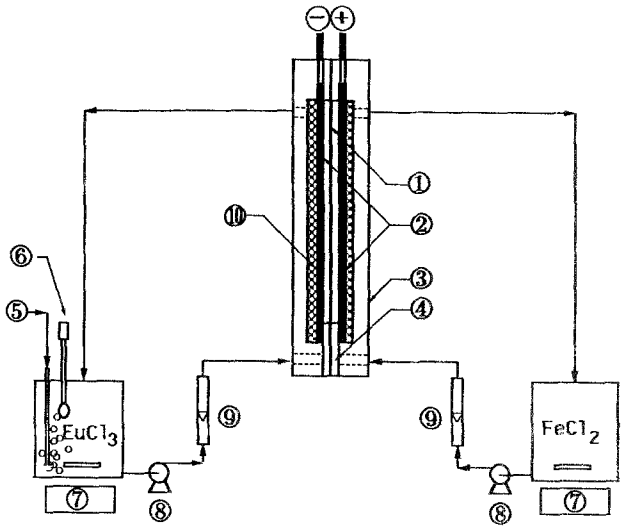

Fig. 1. Schematic diagram of electrolytic reduction of europium in recycling mode. (1) Anion exchange membrane, (2) graphite electrode, (3) acrylic frame, (4) gasket and spacer, (5) Ar-purging tube, (6) pH electrode, (7) magnetic stirrer set, (8) metering pump, (9) flow meter and (10) glass bead.

rubber gasket swathed with Teflon seal tape was placed between the membrane and the electrode plate. The space on the acrylic frame side was filled with glass beads 2.4 mm in diameter to reduce the 'hold up' volume. The cell was assembled using eight threaded steel screws. The electrolyte streams separately flowed from the front face in order to obtain the maximum rate at the front and to minimize the overall ohmic potential drop in solution. The catholyte was composed of lanthanide chloride solution, and the anolyte of ferrous chloride solution. Both streams were pumped and recycled with an FMI metering pump. The flows were measured using microflowmeters. The electrolyte leaving the cell was recycled to a reservoir of volume 0.3 dm^3, which was stirred using a magnetic stirrer. Argon was purged into the catholyte reservoir

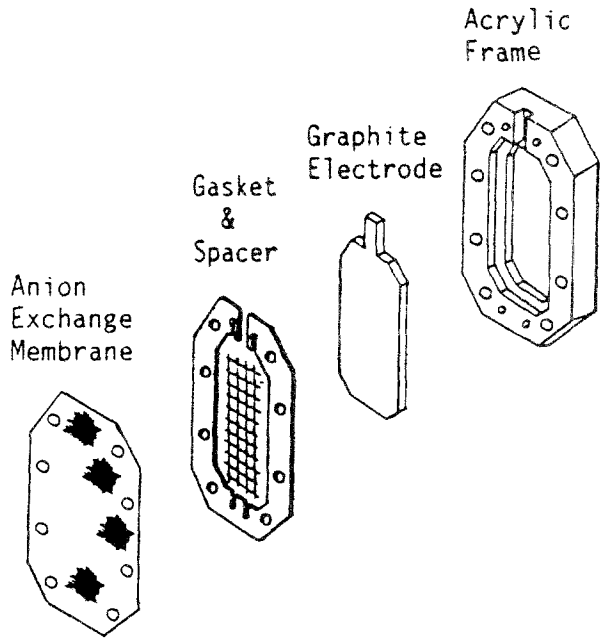

Fig. 2. Assembly of the electrode cell.

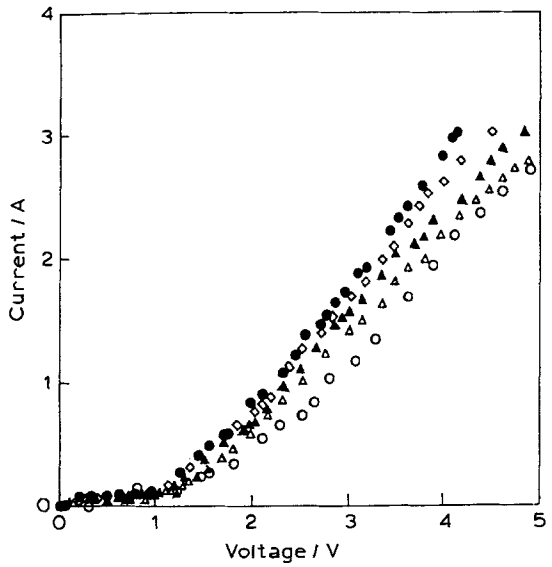

Fig. 3. Current–voltage relationship.

	TRE/M	Eu^{3+}/M	*F.R.*/ *ml min*$^{-1}$
(○)	0.050	0.05	10
(△)	0.465	0.05	5
(▲)	0.465	0.05	10
(◇)	0.465	0.05	15
(●)	0.465	0.05	20

to maintain an oxygen-free environment. The combination pH electrode immersed in the catholyte reservoir was used to monitor and record the pH. Before each run, 300 ml of 0.1 M hydrochloric acid and then deionized water were passed through the cell. All cathodic solution used was first saturated with argon. The anodic feed solution was of 0.3 M ferrous chloride in 0.3 N hydrochloric acid solution.

The electrolysis proceeded at room temperature (about 299 K), galvanostatically using a d.c. power supply. The concentrations of Eu^{2+} and Fe^{2+} were analysed by using the Ce^{4+} titration method with Ferroin as the indicator.

4. Results and discussion

4.1. *Current–voltage relationship*

The relationship between current and cell voltage was measured by simply passing both electrolytes at the same flow rate through the electrodes and continuously varying the cell voltage. The results shown in Fig. 3 indicate that the primary electrolytic reaction began at 1.2 V, which is consistent with the theoretical value given in Equation 4. Figure 3 also shows the effect of flow rate on the current–voltage relation. It is noted that a higher current was detected with higher electrolyte flow rate at a fixed cell voltage, which implies that the electrolytic reaction is diffusion-limited.

4.2. *Effect of lanthanide concentration*

The effect of the total lanthanide concentration

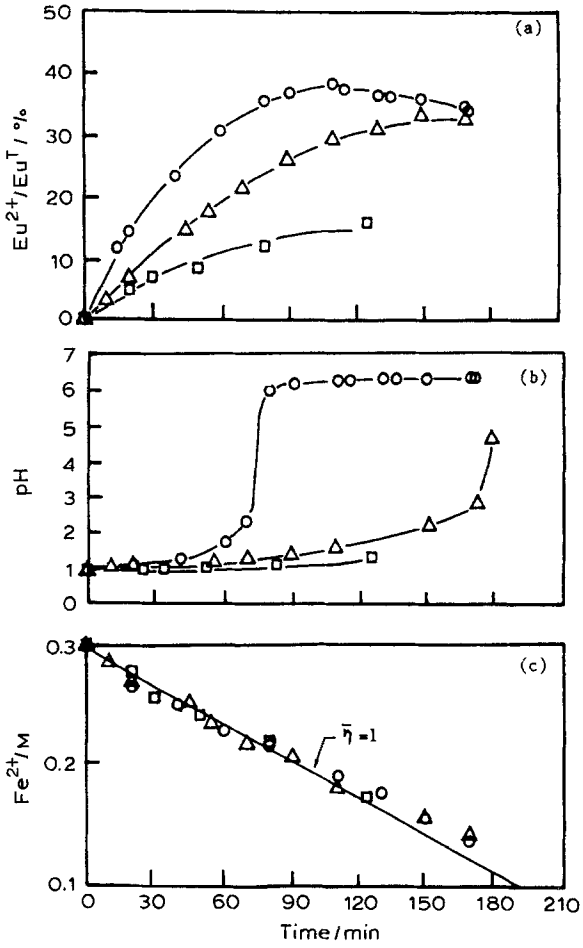

Fig. 4. Effect of lanthanide concentration on (a) Eu reduction and (b) pH variation in cathodic reservoir, and (c) Fe oxidation in anode. Conditions: *F.R.* = 10 ml min^{-1}, I_a = 0.5 A, Eu^{3+} = 0.05 M, pH 1. *TRE* concentration: (○) 0.850, (△) 0.465 and (□) 0.050 M.

(denoted as *TRE*) on the performance of the cell is illustrated in Fig. 4. Figure 4a shows that the rate of europium reduction is higher with higher *TRE* in the feed solution. With various *TRE* concentrations (0.05, 0.465 and 0.85 M), the electric conductivities of electrolytes measured at 298 K are summarized in Table 1. This shows that the electric conductivity increases with increasing *TRE* concentration at pH 1. Although trivalent europium is the only ion which may be reduced in the electrolysis process (as has been discussed previously), other trivalent lanthanides in the feed solution act as supporting electrolyte to reduce the ohmic potential drop through the pore electrolyte.

Figure 4b shows the change of pH in the cathodic reservoir during the course of the experiment. The

Table 1. The electric conductivity of the electrolyte at 298 K and pH 1

Electrolyte TRE conc./M	*Conductivity*/ *S cm*$^{-1}$
0.050	0.096
0.465	0.129
0.850	0.145

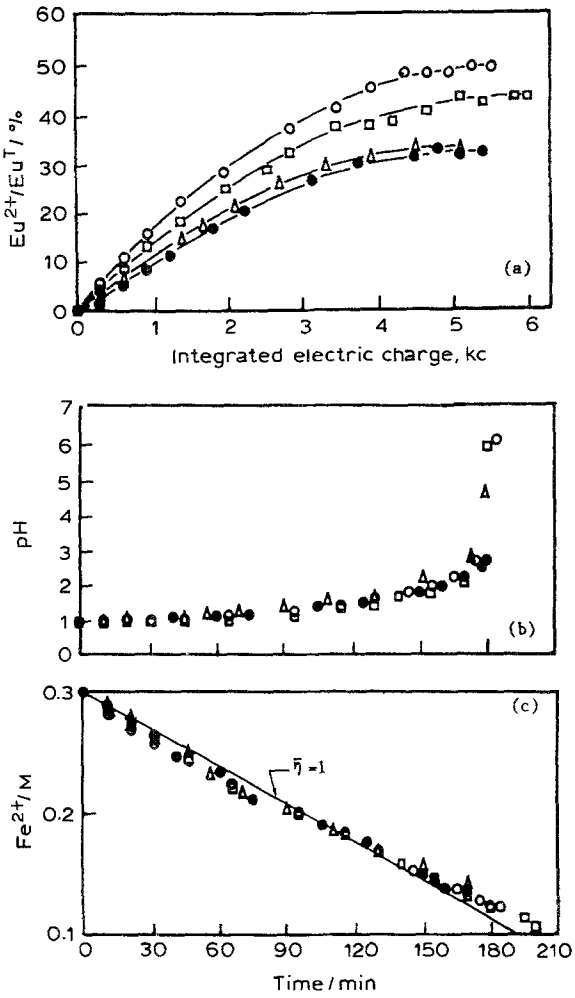

Fig. 5. Influence of flow rate of electrolyte on (a) Eu reduction and (b) pH variation in cathodic reservoir, and (c) Fe oxidation in anode. Conditions: *TRE* concentration = 0.465 M, Eu^{3+} = 0.05 M, pH 1, I_a = 0.5 A. *F.R.*: (●) 5, (△) 10, (□) 15 and (○) 20 ml min^{-1}.

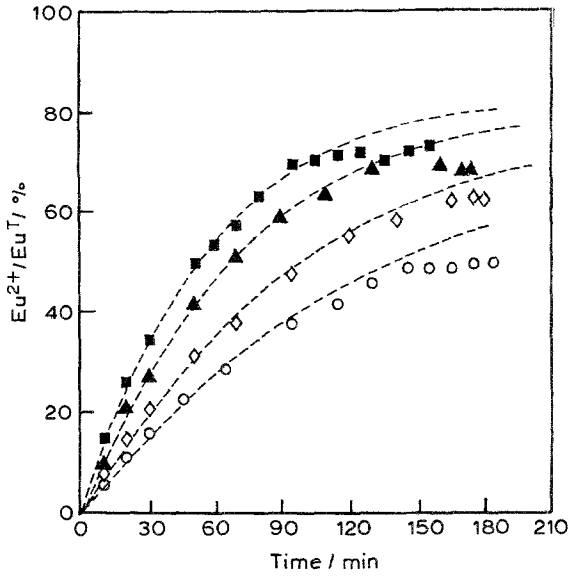

Fig. 6. Europium(II) concentration against time with varying applied current. Initial catholyte: total lanthanide, 0.465 M; europium(III), 0.05 M; pH 1; Q = 20 ml min^{-1}. Current I_a: (■) 1.0, (▲) 0.75, (◇) 0.6 and (○) 0.5 A. (----) Curve fitting with Equation 15.

increase in pH was partially due to hydrogen evolution at the cathode and partially caused by the reoxidation of divalent europium in the reservoir following the Equations 5 and 6. For the experimental run with higher *TRE* concentration (0.85 M) the pH rose steeply to 6 after about 2 h and resulted in the formation of lanthanide hydroxide fouling the electrode, to render the electrolytic cell inoperable. Thus, a high pH must be avoided.

The time-varying anolyte ferrous ion concentration is shown in Fig. 4c. This shows that the total lanthanide concentration of the catholyte does not influence the anodic reaction. All experimental data practically coincide with the theoretical curve calculated by Equation 13 with the mean current efficiency equal to 1. This result indicates that the applied current is less than that corresponding to the limiting current for anodic reaction during most of the experiment.

4.3. *Effect of electrolyte flow rate*

The effect of flow rate on the performance of the cell is shown in Fig. 5. Figure 5a shows the effect on the generation of divalent europium in the cathodic reservoir. This result is attributed to the enhanced convection and the limiting current increased with flow rate. The higher flow rate could also reduce the blanketing effect of surface area due to hydrogen evolution in the electrolyte. The average mass transfer from electrolyte to electrode is undoubtedly increased at higher flow rate.

As shown in Fig. 5b, the flow rate has no significant effect on pH change in the cathodic reservoir. This implies that the hydrogen evolution reaction at the cathode is not concentration dependent. Figure 5c shows that the depletion rate of ferrous ion in the anodic reservoir is not influenced by the flow rate. Almost all data fall on the theoretical line calculated by Equation 13 with $\bar{\eta}$ = 1. This result is similar to that discussed in the previous section.

4.4. *Effect of applied current*

The effect of the applied current on the europium reduction was examined galvanostatically. Figure 6 shows that the concentration of divalent europium increases with time with different applied current. A higher ratio of europium(II) to total europium ions is obtained when a higher current is applied. Nevertheless, the same quantity of europium is reduced with the same quantity of integrated electric charge with both 0.75 A and 1.0 A as shown in Fig. 7a. This implies that a higher current efficiency can be achieved when a higher current is applied, but only up to 0.75 A. Thus an applied current of 0.75 A may be considered as an optimal value. Figure 7b shows that the rate of hydrogen evolution and the measured pH at the cathode both increase with increase in the applied current. With hydrogen evolution at an electrode, gas bubbles substantially reduce the active electrode area, and hence the pore electrolyte resistance is increased. This may result in the absence of any further increase in the current efficiency when the applied current is raised yet higher (as when 1.0 A is applied).

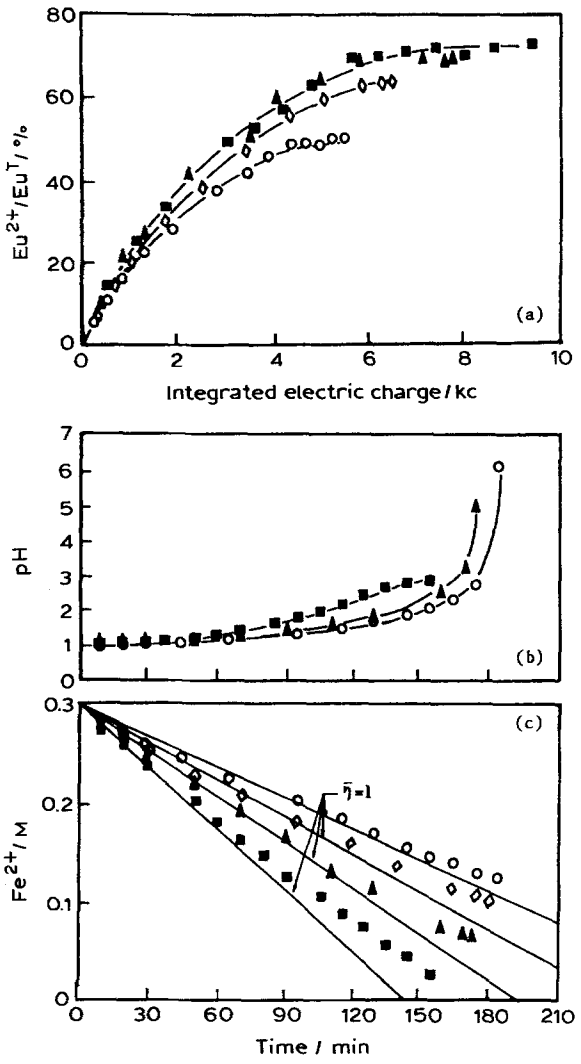

Fig. 7. Effect of applied current on (a) Eu reduction and (b) pH variation in cathodic reservoir, and (c) Fe oxidation in anode. Conditions: *TRE* concentration = 0.465 M, Eu^{3+} = 0.05 M, pH 1, *F.R.* = 20 ml min^{-1}. Current, I_a: (○) 0.5, (◇) 0.6, (▲) 0.75 and (■) 1.0 A.

Figure 7c shows the rate of oxidation of ferrous ion at the anode. A higher rate of anodic reaction was observed with a higher applied current. During recycle, the anodic limiting current decreases and may become smaller than the operating current. Thus the anodic reaction shifts to diffusional control, which leads to a mean current efficiency of less than 1. This effect is more significant with a higher applied current.

4.5. *Comparison between experimental results and theory*

During europium reduction by recycle in the flow-through electrolytic cell, the produced europium(II) may be gradually reoxidized by photo effects and the existence of hydrogen ions. Although a magnetic bar stirring system and argon purging were provided, the total concentration of europium(II) detected in the catholyte reservoir actually decreased with time of operation. Figure 8 shows that the concentration of europium(II) decreases and the amount of reoxidation of europium(II) to europium(III), i.e. $[Eu^{2+}]_i - [Eu^{2+}]$ increases linearly with time. The slope calculated by

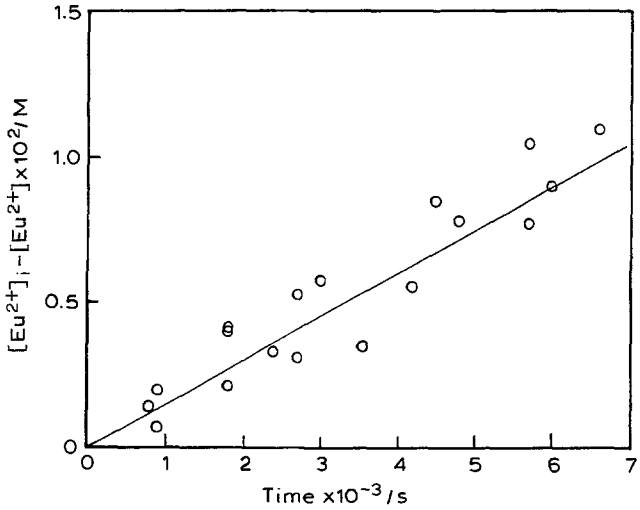

Fig. 8. Relationship between Eu(II) reoxidation and time.

linear regression from experimental data is 1.486 × 10^{-6} mol dm^{-3} s^{-1}. Therefore, zero order kinetics, as assumed previously for europium(II) reoxidation, are verified. The zero order rate constant is thus obtained experimentally, i.e. k = 1.486 × 10^{-6} mol dm^{-3} s^{-1}.

Figure 9 shows the experimental variations of $\bar{\eta}$ (calculated by Equation 13) as a function of the reduced europium concentration for the same experimental conditions as in Fig. 5. For the same europium(II) concentration, a higher mean current efficiency is obtained with a higher flow rate. The dashed lines 1, 2, 3 and 4 denote the theoretical current efficiency calculated by Equation 14 in which the factor f was estimated from the initial reduction rate derived from Equation 11 using the data given in Fig. 5a. The dashed line 5, on the other hand, gives the theoretical current efficiency calculated by combining Equations 16 and 17. This indicates that the europium reduction is under electrochemical control (i.e. $I_a < I_L$) during a period of operating time, when the flow rate is less than 15 ml min^{-1}, and then shifts to diffusional control (i.e. $I_a > I_L$). However, the reaction is all under the

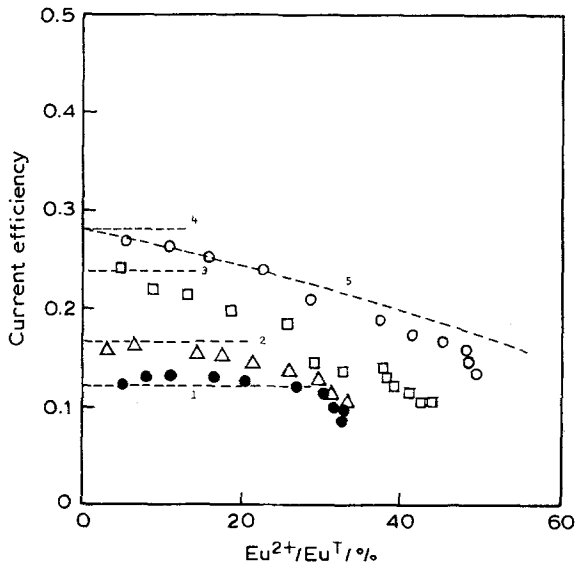

Fig. 9. Mean current efficiency against Eu(II) concentration with varying electrolyte flow rate at I_a = 0.5 A. *F.R.*: (○) 20, (□) 15, (△) 10 and (●) 5 ml min^{-1}. (----) Theoretical curve.

Table 2. Comparison of experiment and calculation for k_a values

Applied current/A	*Experiment*		*Model fitting*	
	R_t	K_a/s^{-1}	R_t	K_a/s^{-1}
0.50	0.115	9.255×10^{-4}	0.109	8.743×10^{-4}
0.60	0.155	1.276×10^{-3}	0.144	1.178×10^{-3}
0.75	0.210	1.786×10^{-3}	0.195	1.643×10^{-3}
1.00	0.270	2.384×10^{-3}	0.242	2.099×10^{-3}

diffusional control from the beginning at the higher flow rate of 20 ml min^{-1}.

Figure 6 shows the relationship between the europium(II) concentration and time in the cathodic reservoir at flow rate 20 ml min^{-1} with different applied currents, I_a = 0.5–1.0 A. Since, at this flow rate, the reduction rate of europium may be diffusion controlled. Equation 16 is used to evaluate the apparent overall mass transfer coefficient $k_a(=k_m a)$ by curve fitting with the experimental data given in Fig. 6. The value of k_a may also be calculated theoretically from experimental data on the conversion factor R_t for a single pass through the electrode. The values of k_a and R_t for operation at $F.R.$ = 20 ml min^{-1} and I_a between 0.5 A and 1.0 A, are summarized in Table 2. It seems reasonable that the values from data fitting are smaller, because these represent the average of the time-dependent data from the recycling operation. The electrochemical application of flow-through porous electrodes has been studied previously [4, 11–14]. The overall mass transfer characteristics actually depend on many factors, for example the type of electrode, reaction kinetics, properties of electrolyte, and electrolyte flow rate, etc. Therefore, the prediction of overall mass transfer coefficients is not a simple matter. The model analysis presented in this study offers a useful method of handling the problem. Table 3 summarizes the various values of k_a reported in the literature.

5. Conclusion

A membrane-partitioned flow-through porous graphite electrode reactor for the study of europium reduction has been experimentally and theoretically examined. High reduction rate and high current efficiency are generally obtained with a high electrolyte flow rate and a charge solution which has a larger lanthanide to europium ratio. Also, high current efficiency is observed with a higher current applied (I_a) when the system involves hydrogen evolution at the cathode. Experimental results indicate that a maximum current efficiency may be obtained with an optimal applied current, I_a = 0.75 A.

Table 3. Comparison of the order of magnitude of k_a with values reported in literature

Type of electrode	*System for treating*	k_a/s^{-1}	*Reference*
Carbon particles (Packed bed)	Cu-removal	4.7×10^{-3}	[11]
Porous carbon	Pb-removal	3.8×10^{-2}	[12]
Carbon particles (Packed bed)	Ag-removal	2.75×10^{-2}	[13]
Porous carbon (Flakes and Chips)	Cu-removal	$3.3 \sim 4.8 \times 10^{-3}$	[14]
Porous graphite	Zn-Cl_2 Battery	$8 \sim 14.4 \times 10^{-2}$	[4]
Porous graphite	Eu-reduction	$0.93 \sim 2.38 \times 10^{-3}$	(This study)

A mathematical model which specifically considered the reoxidation of europium(II) produced a good description of the transient performance characteristics of the system. It is able to picture the electrodynamics of a system involving hydrogen evolution. The model computations compare closely with the experimental results.

Acknowledgement

The part financial support by grant no. NSC77-0402-E007-17 from the National Science Council of Taiwan is gratefully acknowledged.

References

[1] J. S. Newman and W. Tiedemann, 'Advances in Electrochemistry and Electrochemical Engineering', Vol. 11 (edited by H. Gerischer and C. W. Tobias), Wiley, New York (1978) p. 353.
[2] K. Kusakabe, H. Nishida, S. Morooka and Y. Kato, *J. Appl. Electrochem.* **16** (1986) 121.
[3] E. Roayaie and J. Jorne, *J. Electrochem. Soc.* **132** (1985) 1273.
[4] J. Jorne and E. Roayaie, *ibid.* **133** (1986) 696.
[5] E. I. Onstott, US Patent 3 616 326 (1971).
[6] S. J. Dong, Z. X. Li, G. B. Tang, X. L. Zhao, X. Z. Cui and X. W. Yan, *Hua Hueh Tung Pao* **5** (1980) 285.
[7] D. Lu, Y. W. Miao and C. P. Tung, 'Separation Processes in Hydrometallurgy' (edited by G. A. Davies), Ellis Horwood Ltd., England, Chapter 41 (1987) p. 428.
[8] T. Donohue, *Opt. Eng.* **18** (1979) 181.
[9] C. T. Stubblefield and L. Eyring, *J. Am. Chem. Soc.* **77** (1955) 3004.
[10] A. Walker and A. A. Wragg, *Electrochem. Acta* **22** (1977) 1129.
[11] D. N. Bennion and J. Newman, *J. Appl. Electrochem.* **2** (1972) 113.
[12] J. S. Newman and W. Tiedemann, *AIChE J.* **21** (1975) 25.
[13] J. Van Zee and J. Newman, *J. Electrochem. Soc.* **124** (1977) 706.
[14] J. A. Trainham and J. Newman, *ibid.* **124** (1977) 1528.